Archival Report

Biological Psychiatry

Structural Hippocampal Damage Following Anti-*N*-Methyl-D-Aspartate Receptor Encephalitis

Carsten Finke, Ute A. Kopp, Anna Pajkert, Janina R. Behrens, Frank Leypoldt, Jens T. Wuerfel, Christoph J. Ploner, Harald Prüss, and Friedemann Paul

ABSTRACT

BACKGROUND: The majority of patients with anti-*N*-methyl-D-aspartate receptor (NMDAR) encephalitis suffer from persistent memory impairment despite unremarkable routine clinical magnetic resonance imaging. With improved acute care in these patients, neurocognitive impairment represents the major contributor to long-term morbidity and has thus become a focus of attention.

METHODS: Forty patients with anti-NMDAR encephalitis after the acute disease stage and 25 healthy control subjects underwent multimodal structural imaging that combined volumetry of hippocampal subfields with analysis of hippocampal microstructural integrity. Verbal and visuospatial memory performance was assessed in all patients and correlation and mediation analyses were performed to examine associations between hippocampal structural integrity, memory performance, and disease severity.

RESULTS: Hippocampal volumes were significantly reduced in patients and hippocampal subfield analysis revealed bilateral atrophy of the input and output regions of the hippocampal circuit. Microstructural integrity was impaired in both hippocampi in patients. Importantly, hippocampal volumetric and microstructural integrity measures correlated with memory performance and disease severity and duration. Mediation analysis revealed that hippocampal microstructure mediated the effect of disease severity on memory performance.

CONCLUSIONS: Data from this largest cohort of anti-NMDAR encephalitis patients that underwent extensive multimodal magnetic resonance imaging demonstrate that structural hippocampal damage and associated memory deficits are important long-term sequelae of the encephalitis. Correlation with disease duration and severity highlights the need for rapid diagnosis and adequate immunotherapy to prevent persistent damage to the hippocampus. Advanced imaging protocols may allow a more detailed analysis of structural damage to assess disease progression in clinical routine examinations and for therapy evaluation in prospective trials.

Keywords: Autoimmune encephalitis, Hippocampus, Memory, MRI, NMDA, NMDA receptor

http://dx.doi.org/10.1016/j.biopsych.2015.02.024

Anti-*N*-methyl-D-aspartate receptor (NMDAR) encephalitis is a severe autoimmune encephalitis with a characteristic neuropsychiatric clinical syndrome that includes psychiatric symptoms such as psychosis, delusions, and anxiety but also dyskinesia, epileptic seizures, autonomic instability, and disorders of consciousness (1–5). A favorable clinical outcome critically depends on early and aggressive immunotherapy (6). Nevertheless, many patients suffer from long-term cognitive deficits, in particular impairment of memory and executive control, which has become a major determinant of long-term morbidity (2,7). Despite the severity of the disease, routine structural magnetic resonance imaging (MRI) is normal in the majority of patients, even in the acute disease stage. When changes are present, they are typically subtle and may include small white matter lesions that do not correspond to the clinical syndrome (2,3,6). Thus, clinical routine imaging so far has only helped to exclude further differential diagnoses but has not allowed detection of disease-specific structural changes.

Recently, resting state functional MRI analyses revealed reduced functional connectivity of the hippocampus that correlated with individual memory performance in patients with anti-NMDAR encephalitis (8). In addition, smaller hippocampal volumes were observed in patients in comparison with healthy control subjects, however, without significant group differences (8). These findings raised the question whether advanced magnetic resonance analyses could nevertheless detect morphological hippocampal abnormalities reflecting the prolonged clinical deficits, potentially providing novel imaging markers to characterize disease progression and response to therapy. We therefore used a multimodal imaging approach that combined analysis of hippocampal subfield volumes with diffusion tensor imaging derived assessment of hippocampal microstructural integrity in a cohort of 40 well-characterized patients with anti-NMDAR encephalitis. While volumetry of hippocampal subfields allows detection of regional vulnerability to NMDAR antibody-mediated autoimmunity, analysis of hippocampal mean diffusivity (MD) provides a measure of

ISSN: 0006-3223

microstructural integrity that serves as a sensitive marker of structural hippocampal damage (9–11). Furthermore, memory performance was assessed in all patients and correlation analyses were performed between measures of hippocampal structural integrity, memory performance, and disease severity.

METHODS AND MATERIALS

Subjects

Forty patients with anti-NMDAR encephalitis after the acute stage of the disease (36 female patients; mean age ± SEM, 28.0 ± 1.6 years; mean time after disease onset, 26.6 ± 3.3 months) and 25 healthy control subjects without neurological or psychiatric diseases (23 female subjects; mean age ± SEM, 28.1 ± 1.7 years) were included (Table 1). Patients were recruited in Germany and referred to the Department of Neurology, Charité-Universitätsmedizin Berlin. Diagnosis was established in all patients based on characteristic clinical presentation and detection of immunoglobulin G NMDAR antibodies (2). Twelve patients had received drugs with possible neurotoxic side effects, e.g., cyclophosphamide or methotrexate (Supplemental Table S1). Seizures were observed in 31 patients and were rapidly controlled in most cases; for three patients, grand mal seizures series or status epilepticus was reported (Supplemental Table S1). Relapses between disease onset and imaging were observed in four patients. Selected neuropsychological and MRI data analyses of 24 patients have previously been reported (7,8). Two experienced neurologists independently assessed patients' disease severity at the time of study based on the modified Rankin Scale (mRS) (Table 1). Total days spent in acute care hospitals were taken as an estimate of disease duration (Table 1). Control subjects were recruited via public advertisements and had similar social backgrounds in comparison with patients. Premorbid intelligence quotient as assessed using the Mehrfachwahl-Wortschatz-Intelligenztest (an equivalent to the National Adult Reading Test) did not differ significantly between patients and control subjects ($p = .1$). In all subjects, verbal and visuospatial memory performance was assessed using the Rey Auditory Verbal Learning Test (RAVLT) and the Rey-Osterrieth Complex Figure (ROCF). The study was approved by the Charité-Universitätsmedizin Berlin ethics committee. All study participants gave written informed consent.

Table 1. Demographic and Clinical Characteristics

	Patients	Control Subjects
Age (Years; Mean ± SEM [Range])	28.0 ± 1.6 [18–67]	28.1 ± 1.7 [18–61]
Gender	36 female (90%) 4 male (10%)	23 female (92%) 2 male (8%)
mRS (Mean ± SEM [Range])	1.6 ± .2 [0–4]	
Disease Duration[a] (Days; Mean ± SEM [Range])	120 ± 18 [15–410]	
Time After Disease Onset (Months; Mean ± SEM [Range])	26.6 ± 3.3 [1–82]	

mRS, modified Rankin Scale.
[a]Total days in acute care hospitals.

MRI DATA ACQUISITION

Whole-brain MRI data were acquired at the Berlin Center of Advanced Neuroimaging at the Charité on a Siemens Magnetom Tim Trio 3T scanner (Siemens, Erlangen, Germany) using the standard setup for clinical studies with a 12-channel phased-array head coil. High-resolution three-dimensional T1-weighted MRI scans were collected using a magnetization prepared rapid gradient-echo sequence (repetition time = 1900 ms, echo time = 2.55 ms, inversion time = 900 ms, flip angle = 9°, field of view = 240 × 240 mm^2, matrix size = 240 × 240, 176 slices, slice thickness = 1 mm). Diffusion tensor imaging was performed using a single-shot echo-planar imaging sequence (repetition time = 7500 ms, echo time = 86 ms, field of view = 240 × 240 mm^2, voxel size = 2.5 × 2.5 × 2.3 mm^3, 61 slices, 64 diffusion directions, b value = 1000 s/mm^2).

Hippocampal Volumetry and Subfield Segmentation

FreeSurfer (Version 5.1; Center for Biomedical Imaging, Charlestown, Massachusetts) was used to perform hippocampal volumetry, since for quantification of hippocampal volumes FreeSurfer has been found to be more accurate than FSL FIRST (FMRIB, Oxford, United Kingdom) (12) in comparison with manual tracing (13). Moreover, FreeSurfer, but not FSL FIRST, allows analysis of hippocampal subfield volumes. However, for comparison with our previous analysis (8), we also analyzed total hippocampal volumes using FSL FIRST and observed significantly smaller left and right hippocampal volumes in this larger cohort (Supplemental Table S2).

In FreeSurfer, the whole hippocampal formation was first segmented using the standard segmentation pipeline as described in prior publications (14,15). Briefly, this processing includes removal of nonbrain tissue using a hybrid watershed/surface deformation procedure, automated Talairach transformation, and segmentation of the subcortical white matter and deep gray matter volumetric structures, including the hippocampal formation (15,16). Quality control and visual inspection of segmentation results was carried out for all subjects. Next, automated subfield segmentation of the hippocampus was performed using Bayesian inference and a probabilistic atlas of the hippocampal formation based on manual delineations of subfields in ultrahigh T1-weighted scans from control subjects (17,18). The following subfield volumes were calculated: cornu ammonis (CA)1, CA2/3, CA4/dentate gyrus (DG), presubiculum, subiculum, and fimbria (Figure 1). Volumes of the whole hippocampus and hippocampal subfields were adjusted for intracranial volume (ICV) by using the following formula (19):

$$\text{Volume}_{\text{adjusted}} = \text{Volume}_{\text{observed}} - \beta \text{ [slope from ICV vs. regional volume regression]} \times (\text{ICV}_{\text{observed}} - \text{ICV}_{\text{sample mean}})$$

Hippocampal Microstructural Integrity Analysis

Hippocampal microstructure was assessed by diffusion tensor imaging (9–11,20,21). Analyses were performed using FSL 4.1 (FMRIB; www.fmrib.ox.ac.uk/fsl/). Preprocessing of the diffusion tensor imaging data included brain extraction and correction for eddy current distortions. Individual fractional anisotropy and MD maps were calculated by fitting a tensor

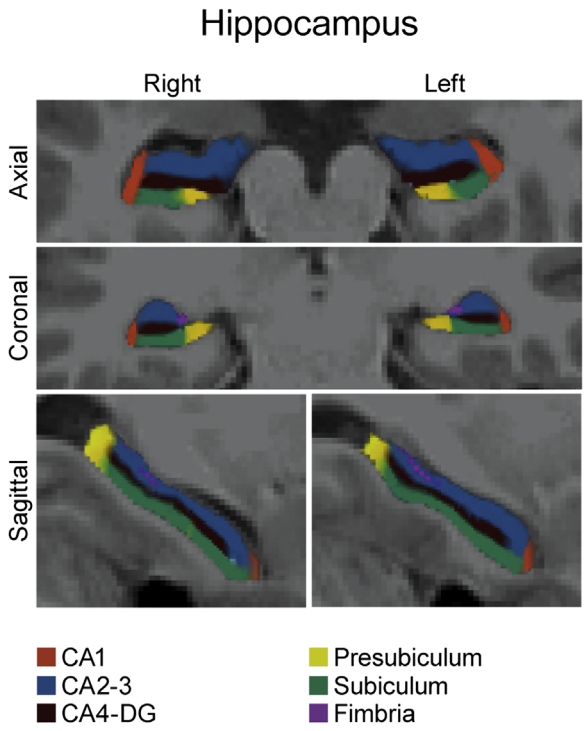

Figure 1. Axial, coronal, and sagittal views of the hippocampal subfields in an example subject. CA, cornu ammonis; DG, dentate gyrus.

model to the diffusion data. Next, individual fractional anisotropy maps were registered to the brain-extracted T1-weighted images using an affine correlation ratio cost function transformation. The resultant transformation matrices were then used for registration of MD maps. FSL FIRST was applied to high-resolution T1-weighted images to obtain individual segmentations of the left and right hippocampus. Results of all registration and segmentation steps were visually inspected for quality control. Finally, hippocampal masks were used for calculation of the mean individual hippocampal MD values.

Statistical Analysis

Statistical analyses were performed using SPSS 21 (IBM, Armonk, New York). Demographic variables and memory performance were compared between groups using independent samples *t* tests and Fisher's exact test for the analysis of gender differences between groups.

To compare hippocampal subfield volumes between patients and control subjects, a multivariate analysis of variance with group as factor and the six subfield volumes as dependent variables was performed. Analyses were conducted separately for left- and right-sided structures. Separate multivariate analyses of variance were used to compare whole left and right hippocampal volume and left and right hippocampal MD between patients and control subjects. Furthermore, hippocampal volumes and MD were compared between patients with and without detectable MRI abnormalities during the acute disease stage and between patients with and without treatment with neurotoxic drugs. To compare the magnitudes of variation between hippocampal subfield volumes, the coefficient of variation was calculated. The coefficient of variation is a standardized measure of variation and is defined as the ratio of the standard deviation to the mean.

Bivariate correlation analyses were performed to analyze whether hippocampal volume and microstructural integrity were associated with memory performance, disease duration and severity, antibody levels, and follow-up time (time between disease onset and study). Furthermore, we analyzed the relationship of follow-up time with clinical (mRS) and cognitive (RAVLT, ROCF) outcome.

Next, we investigated whether hippocampal volume or hippocampal MD indirectly mediates effects of disease severity on memory performance. We therefore performed mediation analyses using a bootstrapping method developed by Hagmann *et al.* (22) implemented in the SPSS toolbox PROCESS (5000 resamples) (23), testing whether the influence of the independent variable X (mRS) on the dependent variable Y (RAVLT sum score or ROCF delayed recall) is mediated by the mediator variable M (total hippocampal volume or hippocampal MD). The indirect effect of X on Y (mediated by M) is considered significant when the bias-corrected 95% confidence interval does not include zero (23).

RESULTS

Patients and control subjects did not differ significantly regarding age ($p = .97$) and gender ($p = 1.0$). Patients had significantly worse verbal and visuospatial memory performance in comparison with control subjects (RAVLT sum score, 57.0 ± 1.9 vs. 65.5 ± 1.4, $p = .001$; ROCF delayed recall, 24.9 ± 1.4 vs. 28.3 ± 1.1, $p = .035$).

Hippocampal Volumetry

Left and right whole hippocampal volumes were reduced in patients relative to control subjects (Figure 2, Table 2). Hippocampal subfield analysis revealed significantly reduced volumes of the left CA4/DG region, fimbria, presubiculum, and subiculum. For the right hippocampus, analysis showed reduced volumes of CA1, CA2/3, CA4/DG, presubiculum, and subiculum (Figure 2, Table 2). In patients, verbal memory performance (RAVLT sum score) correlated with total left hippocampal volume ($r = .450$, $p = .005$; Figure 3) and with volumes of the left CA2/3 region ($r = .339$, $p = .040$), CA4/DG region ($r = .420$, $p = .010$), and presubiculum ($r = .396$, $p = .015$) but not with right hippocampal volumes (all $r < .3$, all $p > .07$). Furthermore, disease severity predicted left hippocampal volume ($r = -.430$, $p = .006$; Figure 3), left CA4/DG ($r = -.343$, $p = .019$), and left subiculum ($r = -.368$, $p = .019$) volumes. Disease duration correlated with total left hippocampal volume ($r = -.347$, $p = .035$). No significant correlations of hippocampal volumes with visuospatial memory performance (ROCF delayed recall) were observed. In control subjects, no significant correlations between hippocampal volumes and memory performance were observed. Coefficients of variation were comparable for all subfields and did not differ between significant and nonsignificant subfield group comparisons (.11–.36 vs. .09–.33; $p = .49$).

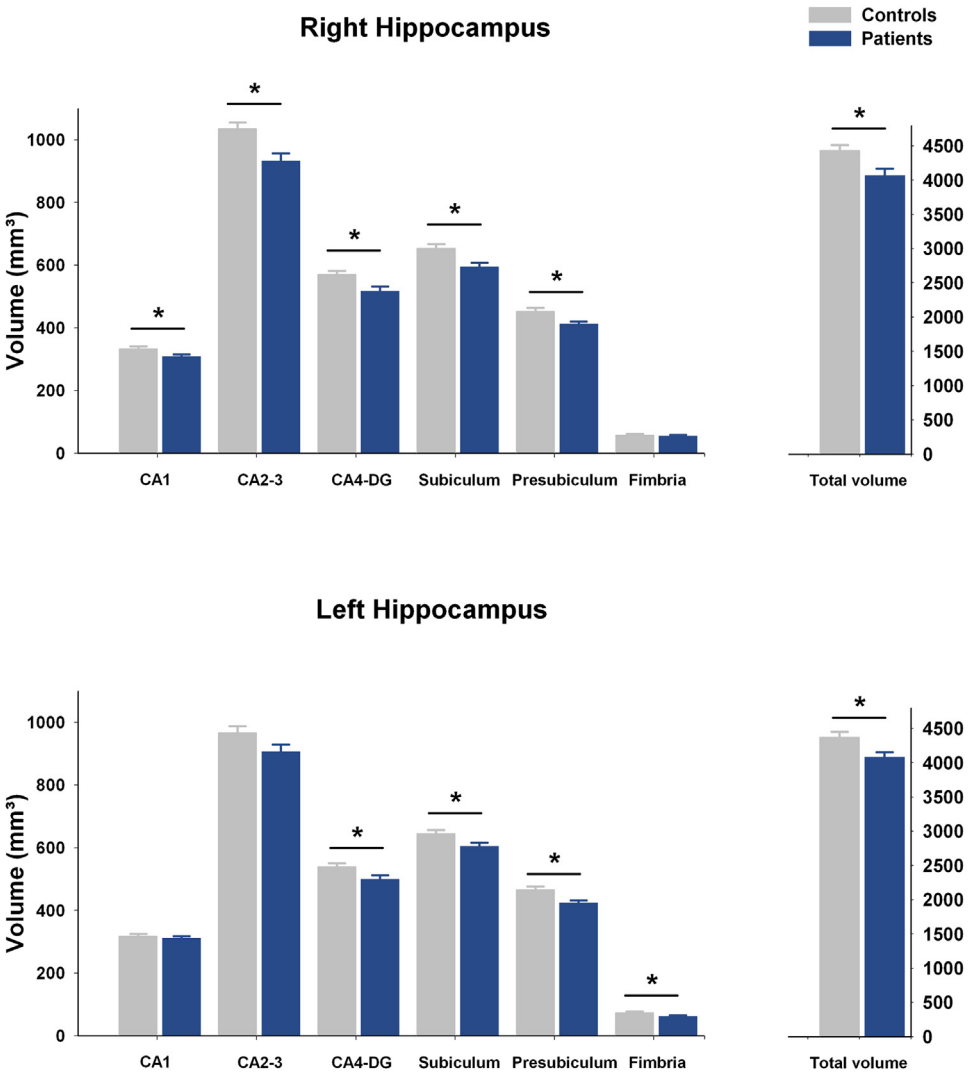

Figure 2. Volumes of the hippocampal subfields and the whole hippocampi in patients and control subjects (mean ± SEM; *$p < .05$). CA, cornu ammonis; DG, dentate gyrus.

Hippocampal Microstructure

Patients showed increased left and right hippocampal mean diffusivity relative to control subjects (Figure 4, Table 3), indicating reduced microstructural integrity of both hippocampi (24). Left and right hippocampal MD correlated with verbal memory performance (RAVLT sum score; left, $r = -.524$, $p = .001$; right, $r = -.470$, $p = .004$; Figure 3) and visuospatial memory performance (ROCF delayed recall; left $r = -.45$, $p = .008$; right, $r = -.44$, $p = .009$) in patients. Disease severity and duration correlated with left ($r = .432/.446$, $p = .007/.007$) and right ($r = .355/.347$, $p = .029/.041$) hippocampal MD (Figure 3). In control subjects, no significant correlations between hippocampal MD and memory performance were observed.

Longer follow-up was associated with better clinical outcome (mRS; $r = -.34$, $p = .037$) but not with memory performance (RAVLT sum score, $p = .18$; ROCF delayed recall, $p = .82$) or hippocampal volumes or MD (all $p > .12$). Serum and cerebrospinal fluid antibody levels did not correlate significantly with structural hippocampal measures or memory performance. No significant differences of hippocampal volumes and/or hippocampal MD between patients with and without detectable MRI abnormalities during the acute disease stage and between patients with and without treatment with neurotoxic drugs were observed.

Mediation Analysis

Mediation analysis revealed that left hippocampal MD partially mediated the effect of disease severity (mRS) on memory performance (RAVLT sum score), i.e., a significant indirect effect of mRS on RAVLT performance was observed (b = −1.639, 95% bias-corrected bootstrap confidence interval [−5.306, −.073]) with an effect size of $\kappa^2 = .158$ (95% bias-corrected bootstrap confidence interval [.013, .398]). No significant mediation was observed for models including right hippocampal MD and hippocampal volume as mediator variables and models including ROCF as dependent variable.

Table 2. Whole Hippocampus and Hippocampal Subfield Volumes

	Patients			Control Subjects				
	Mean	SEM	CV	Mean	SEM	CV	*F*	*p* Value
Left								
CA1	311.92	6.07	.12	319.08	8.11	.13	.512	.477
CA2-3	907.59	22.23	.15	968.45	20.81	.11	3.483	.067
CA4-DG	500.51	11.35	.14	541.33	11.06	.10	5.884	.018
Fimbria	62.78	3.00	.30	74.87	4.89	.33	4.984	.029
Presubiculum	424.77	7.30	.11	468.17	10.48	.11	12.24	.001
Subiculum	605.00	11.45	.12	646.54	11.73	.09	5.828	.019
Hippocampus	4083.61	72.72	.11	4385.99	77.51	.09	7.477	.008
Right								
CA1	308.75	6.63	.14	334.86	7.54	.11	6.437	.014
CA2-3	932.88	24.46	.17	1036.18	21.25	.10	8.588	.005
CA4-DG	518.07	13.37	.16	571.63	11.55	.10	7.747	.007
Fimbria	56.11	2.61	.29	58.50	4.22	.36	.258	.613
Presubiculum	412.42	7.97	.12	453.26	12.06	.13	8.674	.005
Subiculum	595.18	12.63	.13	655.29	13.29	.10	9.863	.003
Hippocampus	4069.83	101.20	.16	4441.80	81.32	.09	6.724	.012

CA, cornu ammonis; CV, coefficient of variation; DG, dentate gyrus.

DISCUSSION

Our study demonstrates hippocampal subfield atrophy and impaired microstructural integrity of the hippocampus in a sample of 40 patients recovering from anti-NMDAR encephalitis. Importantly, volumetric and microstructural integrity measures correlated with memory performance and disease severity and duration. We thus describe a structural imaging correlate of anti-NMDAR encephalitis that provides insights into the pathophysiology of the disease and that may serve as a therapeutic and prognostic biomarker.

The majority of patients with anti-NMDAR encephalitis achieve a good clinical outcome, especially with rapid immunotherapy and tumor removal (6). However, most patients suffer from long-lasting cognitive deficits, in particular memory impairments and executive dysfunction (7). We have previously shown reduced functional connectivity between the anterior hippocampus and the medial prefrontal cortex that correlated with individual memory performance despite normal routine clinical MRI and gray matter morphology (8). Here, we analyzed hippocampal structural integrity using a refined analysis strategy that included study of hippocampal subfield volumes and hippocampal MD (13,17). Hippocampal volumetry revealed atrophy of the left and right whole hippocampus with bilateral affection of CA4/DG, subiculum, and presubiculum in anti-NMDAR encephalitis patients that had recovered from the acute disease stage. In the right hippocampus, atrophy also included CA1 and CA2/3 subfields, whereas in the left hippocampus, fimbria volume was additionally reduced. Volumes of the left whole hippocampus and left CA2/3, CA4/DG, and presubiculum correlated with verbal memory performance, reflecting the material specificity of the left hippocampus for verbal stimuli. The dentate gyrus, affected bilaterally in patients, serves as the major input to the hippocampus and receives projections mainly from the entorhinal cortex (25). It is thought to prepare incoming information for efficient storage and is involved in pattern separation, a process that enables the formation of discrete memory representations (26). Importantly, the dentate gyrus is one of a few brain regions exhibiting adult neurogenesis with the newly generated neurons critically enhancing accuracy of memory encoding by contributing to pattern separation (27). From the dentate gyrus, information flows to CA2/3, CA1, subiculum/presubiculum, and then back to the entorhinal cortex (25). Subiculum and presubiculum, also bilaterally affected in patients, are part of the subicular complex. Both structures form the major output structures of the hippocampus and support the retrieval of encoded information (26). Hence, subfield atrophy that was bilaterally present in anti-NMDAR encephalitis affected both the major input and the major output structures of the hippocampal circuit.

Previous analyses of hippocampal subfield volumes in patients with memory disorders identified comparable atrophy patterns. Patients with mild cognitive impairment showed a correlation of memory performance with CA2/3, CA4/DG, and subicular volumes (18). Volumes of the left CA2/3 and CA4/DG correlated with verbal memory performance in patients with self-reported memory deficits (28). In patients with Parkinson's disease, CA2/3 and CA4/DG volumes were reduced and also correlated with verbal memory performance (29). Interestingly, a recent histopathologic study in epilepsy patients undergoing selective amygdalohippocampectomy showed that patients with predominant cell loss in CA1 did not show declarative memory impairment, while patients with neuronal loss affecting CA4 and dentate gyrus had significantly impaired declarative memory (30). Thus, bilateral affection of CA4/DG and subiculum is well suited to explain the sustained memory deficits observed in anti-NMDAR encephalitis.

We extended the findings on hippocampal subfield volumetry by analyzing hippocampal MD that reflects hippocampal microstructural integrity (21,24). Specifically, MD is a measure of the mean motion of water molecules in tissue and is derived from diffusion tensor imaging. Intact membranes and tissue cytoarchitecture impose natural limits to diffusion and MD increases indicate expansion of extracellular fluid and microscopic barrier disruption and are thus considered as a measure of neuronal disintegration (24,31,32). Previous studies observed an association between lower hippocampal MD and better memory performance in healthy older individuals (11,21), while spatial navigation training led to a reduction in hippocampal MD paralleled by improved navigation performance (24). Moreover, increased hippocampal MD is associated with an increased risk of progression to Alzheimer's disease in patients with amnestic mild cognitive impairment (33). A recent study furthermore reported that higher glucose levels are correlated with increased hippocampal MD and impaired verbal memory performance in healthy older subjects (10). In the present study, MD was significantly increased in the left and right hippocampus of patients with anti-NMDAR encephalitis indicating impaired microstructural integrity. Moreover, left and right hippocampal MD correlated with verbal and visuospatial memory performance.

Our results demonstrate that patients with anti-NMDAR encephalitis suffer from long-standing structural damage to the hippocampus, i.e., reduced volumes of hippocampal input and output structures and impaired microstructural integrity. Moreover, these structural changes are clinically relevant given

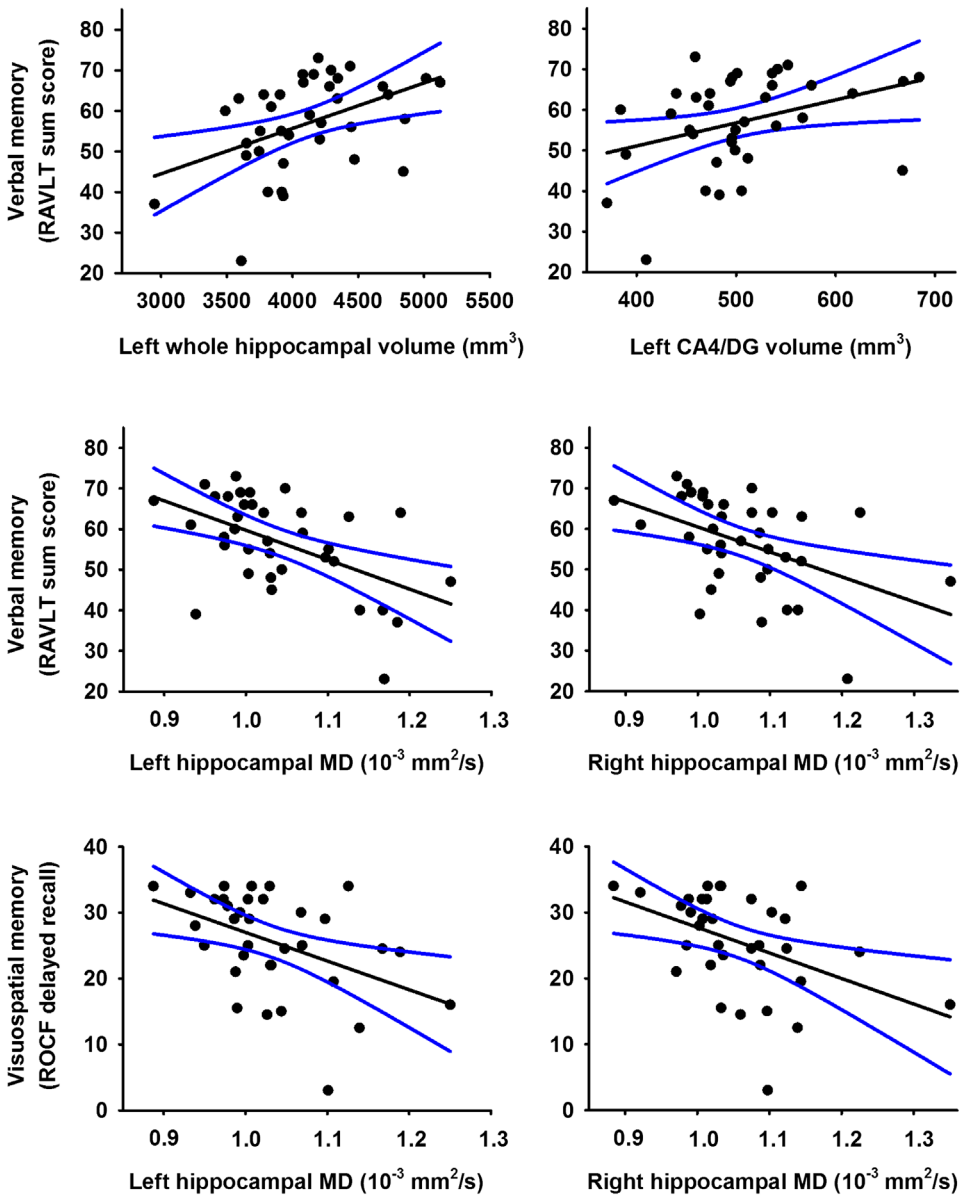

Figure 3. Correlations of hippocampal volumes and mean diffusivity (MD) with verbal and visuospatial memory performance. CA, cornu ammonis; DG, dentate gyrus; RAVLT, Rey Auditory Verbal Learning Test; ROCF, Rey-Osterrieth Complex Figure.

their strong correlation with memory performance. These observations herald important implications for the pathophysiological concept of the disease and for the clinical management of patients. Extending the previous observation of reduced functional connectivity of the hippocampus, our data support the notion that the hippocampus is one of the target structures of the disease (8). This notion is in line with evidence that the hippocampus contains the highest density of NMDAR in the brain and that dysfunction of hippocampal NMDAR causes severe amnesia (34,35). Moreover, the detection of persistent structural damage also points to the presence of pathophysiological mechanisms that go beyond the established antibody-mediated capping and internalization of NMDARs causing reversible impairment of NMDAR-mediated synaptic function without cell death (36,37). Interestingly, the observed hippocampal atrophy pattern was slightly asymmetric. This is in line with previous positron emission tomography imaging studies showing widespread hemispheric asymmetries (38–40). Like in other autoimmune diseases of the nervous system, neurological deficits are not necessarily symmetric in anti-NMDAR encephalitis. Recently, it has been proposed that left-right asymmetry is a fundamental property of the mammalian hippocampus, based on observations that NMDAR subunits are differentially distributed between the left and right mouse hippocampus and that hippocampal CA1 pyramidal cell synapses differ in NMDAR expression depending on the laterality of presynaptic origin (41,42). Moreover, asymmetry was also reported for

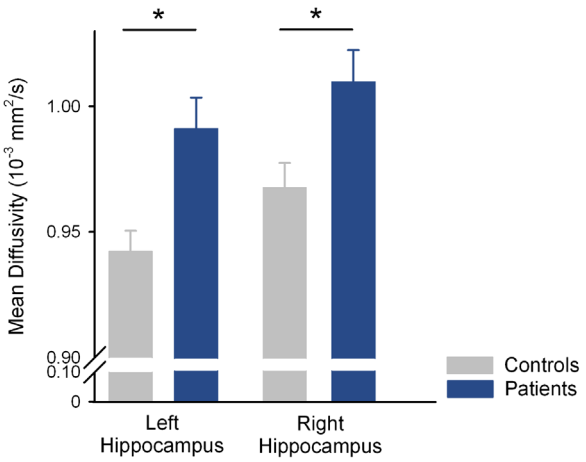

Figure 4. Hippocampal mean diffusivity in patients and control subjects (mean ± SEM; *$p < .05$).

hippocampal synaptic plasticity and was thought to rely on the differential expression of NMDAR subunits (43). Whether such an asymmetry of NMDAR expression likewise exists in the human hippocampus and how this relates to pathophysiological processes in NMDAR encephalitis needs to be determined in future studies. On clinical grounds, detection of hippocampal damage explains the frequent observation of long-term cognitive deficits following anti-NMDAR encephalitis that constitute the chief complaint affecting daily life of patients (7). Importantly, our data show correlation of disease severity and disease duration with microstructural integrity of both hippocampi and with volumes of the left whole hippocampus, left CA4/DG, and left subiculum. Mediation analysis furthermore revealed that left hippocampal microstructural integrity partially mediated the effect of disease severity on memory performance, thus showing that more severe disease courses lead to more pronounced structural deficits that, in turn, are associated with worse memory performance. In line with previous analyses, longer follow-up after the acute disease stage was associated with better clinical outcome reflected in better mRS scores. These results indicate that the recovery process in anti-NMDAR encephalitis is slow and suggests potential for continuing clinical improvement in these patients. However, we observed no significant correlation of follow-up time with memory performance or structural hippocampal measures, illustrating a limited capacity for the compensation of memory deficits. These results stress the relevance of rapid diagnosis and early and adequate immunotherapy to prevent hippocampal damage and to improve the cognitive long-term outcome of patients (7). This is in keeping with clear evidence of better outcome in patients with shorter time until treatment initiation and in patients switched to second-line immunotherapy who did not respond to first-line treatment (6,7).

Table 3. Left and Right Hippocampal Mean Diffusivity

	Patients		Control Subjects				
	Mean	SEM	Mean	SEM	*df*	*F*	*p* Value
Left MD	.9913	.0123	.9424	.0081	1	8.888	.004
Right MD	1.0099	.0126	.9678	.0099	1	5.862	.019

MD, mean diffusivity.

Limitations of the study include employment of a processing pipeline that does not discriminate hippocampal subfields CA2 from CA3 and CA4 from dentate gyrus. Advances in imaging acquisition and segmentation algorithms will likely allow for such analyses in future studies of healthy subjects and patients with medial temporal lobe pathologies. Treatment with neurotoxic drugs and longstanding seizures potentially can contribute to cerebral atrophy. However, we observed no differences in structural hippocampal measures between patients with and without treatment with neurotoxic drugs. Furthermore, in most of our patients, only few seizures occurred that were rapidly controlled, making a contribution of seizures to long-lasting hippocampal damage unlikely. Longitudinal studies are needed to assess whether cognitive deficits further improve after longer follow-up periods and how continued recovery is related to structural alterations of the hippocampus. Magnetic resonance spectroscopy investigations might moreover elucidate how functional and structural MRI changes relate to cerebral glutamate levels in patients with anti-NMDAR encephalitis.

Our study demonstrates that patients with anti-NMDAR encephalitis exhibit relevant and long-standing structural damage of the hippocampus. Disease severity and duration predicted the extent of hippocampal damage that, in turn, correlated with memory performance. Together with previous observations (6,7), these results call for rapid diagnosis and efficient immunotherapy to prevent cognitive long-term deficits. Moreover, the results provide a focal structural imaging biomarker of the disease that may support treatment decisions and prognostic evaluation.

ACKNOWLEDGMENTS AND DISCLOSURES

This study was supported by the German Research Council (Grant Nos. DFG Exc 257 to FP, DFG PR 1274/2-1 to HP, and DFG PI 248/4-1 to CJP).

The authors report no biomedical financial interests or potential conflicts of interest.

ARTICLE INFORMATION

From the Department of Neurology (CF, UAK, AP, CJP, HP, FP), Berlin Center for Advanced Neuroimaging (CF, JRB, FP), and Neurocure Clinical Research Center (JRB, JTW, FP), Charité–Universitätsmedizin Berlin, Berlin; Berlin School of Mind and Brain (CF), Humboldt-Universität zu Berlin; Neuroimmunology Unit (FL), Clinical Chemistry and Neurology, University Hospital Schleswig-Holstein, Kiel; Institute of Neuroradiology (JTW), University Medicine Goettingen, Goettingen; and Experimental and Clinical Research Center (JTW, FP), Charité–Universitätsmedizin Berlin; Max Delbrueck Center for Molecular Medicine (JTW, FP); German Center for Neurodegenerative Diseases (HP); and Clinical and Experimental Multiple Sclerosis Research Center (FP), Charité–Universitätsmedizin Berlin, Berlin, Germany.

HP and FP contributed equally to this work.

Address correspondence to Carsten Finke, M.D., Charité–Universitätsmedizin Berlin, Department of Neurology, Charitéplatz 1, Berlin 10117, Germany; E-mail: carsten.finke@charite.de.

Received Oct 27, 2014; revised Feb 6, 2015; accepted Feb 18, 2015.

Supplementary material cited in this article is available online at http://dx.doi.org/10.1016/j.biopsych.2015.02.024.

REFERENCES

1. Dalmau J, Gleichman AJ, Hughes EG, Rossi JE, Peng X, Lai M, *et al*. (2008): Anti-NMDA-receptor encephalitis: Case series and analysis of the effects of antibodies. Lancet Neurol 7:1091–1098.
2. Dalmau J, Lancaster E, Martinez-Hernandez E, Rosenfeld MR, Balice-Gordon R (2011): Clinical experience and laboratory investigations in patients with anti-NMDAR encephalitis. Lancet Neurol 10:63–74.
3. Irani SR, Bera K, Waters P, Zuliani L, Maxwell S, Zandi MS, *et al*. (2010): N-methyl-D-aspartate antibody encephalitis: Temporal progression of clinical and paraclinical observations in a predominantly non-paraneoplastic disorder of both sexes. Brain 133:1655–1667.
4. Viaccoz A, Desestret V, Ducray F, Picard G, Cavillon G, Rogemond V, *et al*. (2014): Clinical specificities of adult male patients with NMDA receptor antibodies encephalitis. Neurology 82:556–563.
5. Deakin J, Lennox BR, Zandi MS (2014): Antibodies to the N-methyl-D-aspartate receptor and other synaptic proteins in psychosis. Biol Psychiatry 75:284–291.
6. Titulaer MJ, McCracken L, Gabilondo I, Armangué T, Glaser C, Iizuka T, *et al*. (2013): Treatment and prognostic factors for long-term outcome in patients with anti-NMDA receptor encephalitis: An observational cohort study. Lancet Neurol 12:157–165.
7. Finke C, Kopp UA, Prüss H, Dalmau J, Wandinger K-P, Ploner CJ (2012): Cognitive deficits following anti-NMDA receptor encephalitis. J Neurol Neurosurg Psychiatry 83:195–198.
8. Finke C, Kopp UA, Scheel M, Pech L-M, Soemmer C, Schlichting J, *et al*. (2013): Functional and structural brain changes in anti-N-methyl-D-aspartate receptor encephalitis. Ann Neurol 74:284–296.
9. Pereira JB, Valls-Pedret C, Ros E, Palacios E, Falcón C, Bargalló N, *et al*. (2014): Regional vulnerability of hippocampal subfields to aging measured by structural and diffusion MRI. Hippocampus 24:403–414.
10. Kerti L, Witte AV, Winkler A, Grittner U, Rujescu D, Flöel A (2013): Higher glucose levels associated with lower memory and reduced hippocampal microstructure. Neurology 81:1746–1752.
11. Carlesimo GA, Cherubini A, Caltagirone C, Spalletta G (2010): Hippocampal mean diffusivity and memory in healthy elderly individuals: A cross-sectional study. Neurology 74:194–200.
12. Patenaude B, Smith SM, Kennedy DN, Jenkinson M (2011): A Bayesian model of shape and appearance for subcortical brain segmentation. Neuroimage 56:907–922.
13. Morey RA, Petty CM, Xu Y, Hayes JP, Wagner HR, Lewis DV, *et al*. (2009): A comparison of automated segmentation and manual tracing for quantifying hippocampal and amygdala volumes. Neuroimage 45:855–866.
14. Fischl B, Salat DH, Busa E, Albert M, Dieterich M, Haselgrove C, *et al*. (2002): Whole brain segmentation: Automated labeling of neuroanatomical structures in the human brain. Neuron 33:341–355.
15. Fischl B, Salat DH, van der Kouwe AJW, Makris N, Ségonne F, Quinn BT, Dale AM (2004): Sequence-independent segmentation of magnetic resonance images. Neuroimage 23(suppl 1):S69–S84.
16. Ségonne F, Dale AM, Busa E, Glessner M, Salat D, Hahn HK, Fischl B (2004): A hybrid approach to the skull stripping problem in MRI. Neuroimage 22:1060–1075.
17. Van Leemput K, Bakkour A, Benner T, Wiggins G, Wald LL, Augustinack J, *et al*. (2009): Automated segmentation of hippocampal subfields from ultra-high resolution in vivo MRI. Hippocampus 19:549–557.
18. Hanseeuw BJ, Van Leemput K, Kavec M, Grandin C, Seron X, Ivanoiu A (2011): Mild cognitive impairment: Differential atrophy in the hippocampal subfields. AJNR Am J Neuroradiol 32:1658–1661.
19. Buckner RL, Head D, Parker J, Fotenos AF, Marcus D, Morris JC, Snyder AZ (2004): A unified approach for morphometric and functional data analysis in young, old, and demented adults using automated atlas-based head size normalization: Reliability and validation against manual measurement of total intracranial volume. Neuroimage 23:724–738.
20. Péran P, Cherubini A, Assogna F, Piras F, Quattrocchi C, Peppe A, *et al*. (2010): Magnetic resonance imaging markers of Parkinson's disease nigrostriatal signature. Brain 133:3423–3433.
21. Den Heijer T, der Lijn F Van, Vernooij MW, de Groot M, Koudstaal PJ, der Lugt Av, *et al*. (2012): Structural and diffusion MRI measures of the hippocampus and memory performance. Neuroimage 63:1782–1789.
22. Preacher KJ, Hayes AF (2004): SPSS and SAS procedures for estimating indirect effects in simple mediation models. Behav Res Methods Instrum Comput 36:717–731.
23. Hayes AF (2013): Introduction to Mediation, Moderation, and Conditional Process Analysis: A Regression-Based Approach. New York: Guilford Press.
24. Lövdén M, Schaefer S, Noack H, Bodammer NC, Kühn S, Heinze H-J, *et al*. (2012): Spatial navigation training protects the hippocampus against age-related changes during early and late adulthood. Neurobiol Aging 33;620.e9–620.e22.
25. Insausti R, Amaral DG (2004): Hippocampal formation. In: Paxinos G, Mai J, editors. The Human Nervous System. Amsterdam: Elsevier Academic Press, 871–915.
26. Andersen P, Morris R, Amaral D, Bliss T, O'Keefe J (Eds.) (2007). The Hippocampus Book. Oxford, UK: Oxford University Press.
27. Clelland CD, Choi M, Romberg C, Clemenson GD, Fragniere A, Tyers P, *et al*. (2009): A functional role for adult hippocampal neurogenesis in spatial pattern separation. Science 325:210–213.
28. Engvig A, Fjell AM, Westlye LT, Skaane NV, Sundseth Ø, Walhovd KB (2012): Hippocampal subfield volumes correlate with memory training benefit in subjective memory impairment. Neuroimage 61:188–194.
29. Pereira JB, Junqué C, Bartrés-Faz D, Ramírez-Ruiz B, Marti M-J, Tolosa E (2013): Regional vulnerability of hippocampal subfields and memory deficits in Parkinson's disease. Hippocampus 728:720–728.
30. Coras R, Pauli E, Li J, Schwarz M, Rössler K, Buchfelder M, *et al*. (2014): Differential influence of hippocampal subfields to memory formation: Insights from patients with temporal lobe epilepsy. Brain 137:1945–1957.
31. Le Bihan D, Mangin JF, Poupon C, Clark CA, Pappata S, Molko N, Chabriat H (2001): Diffusion tensor imaging: Concepts and applications. J Magn Reson Imaging 13:534–546.
32. Beaulieu C (2002): The basis of anisotropic water diffusion in the nervous system - a technical review. NMR Biomed 15:435–455.
33. Kantarci K, Petersen RC, Boeve BF, Knopman DS, Weigand SD, O'Brien PC, *et al*. (2005): DWI predicts future progression to Alzheimer disease in amnestic mild cognitive impairment. Neurology 64:902–904.
34. Monaghan DT, Cotman CW (1985): Distribution of N-methyl-D-aspartate-sensitive L-[3H]glutamate-binding sites in rat brain. J Neurosci 5:2909–2919.
35. Nakazawa K, McHugh TJ, Wilson MA, Tonegawa S (2004): NMDA receptors, place cells and hippocampal spatial memory. Nat Rev Neurosci 5:361–372.
36. Hughes EG, Peng X, Gleichman AJ, Lai M, Zhou L, Tsou R, *et al*. (2010): Cellular and synaptic mechanisms of anti-NMDA receptor encephalitis. J Neurosci 30:5866–5875.
37. Moscato EH, Peng X, Jain A, Parsons TD, Dalmau J, Balice-Gordon RJ (2014): Acute mechanisms underlying antibody effects in anti-N-methyl-D-aspartate receptor encephalitis. Ann Neurol 76:108–119.
38. Leypoldt F, Buchert R, Kleiter I, Marienhagen J, Gelderblom M, Magnus T, *et al*. (2012): Fluorodeoxyglucose positron emission tomography in anti-N-methyl-D-aspartate receptor encephalitis: Distinct pattern of disease. J Neurol Neurosurg Psychiatry 83:681–686.
39. Wegner F, Wilke F, Raab P, Tayeb S Ben, Boeck A, Haense C, *et al*. (2014): Anti-leucine rich glioma inactivated 1 protein and anti-N-methyl-D-aspartate receptor encephalitis show distinct patterns of brain glucose metabolism in 18F-fluoro-2-deoxy-d-glucose positron emission tomography. BMC Neurol 14:136.
40. Baumgartner A, Rauer S, Mader I, Meyer PT (2013): Cerebral FDG-PET and MRI findings in autoimmune limbic encephalitis: Correlation with autoantibody types. J Neurol 260:2744–2753.
41. Kawakami R, Shinohara Y, Kato Y, Sugiyama H, Shigemoto R, Ito I (2003): Asymmetrical allocation of NMDA receptor epsilon2 subunits in hippocampal circuitry. Science 300:990–994.
42. Shinohara Y, Hirase H, Watanabe M, Itakura M, Takahashi M, Shigemoto R (2008): Left-right asymmetry of the hippocampal synapses with differential subunit allocation of glutamate receptors. Proc Natl Acad Sci U S A 105:19498–19503.
43. Kohl MM, Shipton OA, Deacon RM, Rawlins JNP, Deisseroth K, Paulsen O (2011): Hemisphere-specific optogenetic stimulation reveals left-right asymmetry of hippocampal plasticity. Nat Neurosci 14:1413–1415.